

CHAPTER V
NON-ISOTHERMAL MELT CRYSTALLIZATION KINETICS FOR
ETHYLENE-ACRYLIC ACID COPOLYMERS AND ETHYLENE-METHYL
ACRYLATE-ACRYLIC ACID TERPOLYMERS

Nathaporn Somrang,^a Manit Nithitanakul,^{1,a} Pitt Supaphol,^{2,a} and Brian P. Grady^b

^aThe Petroleum and Petrochemical College, Chulalongkorn University, Bangkok, THAILAND

^bSchool of Chemical Engineering and Materials Science, The University of Oklahoma, Norman, USA

ABSTRACT

The non-isothermal melt crystallization kinetics and subsequent melting behavior for four different grades of ethylene-acrylic acid copolymer and three different grades of ethylene-methyl acrylate-acrylic acid terpolymer was investigated by the differential scanning calorimetry technique. The non-isothermal melt crystallization data were analyzed based on the Ozawa and Ziabicki macrokinetic models. The effective energy barriers describing non-isothermal melt crystallization process for these resins were determined based on the differential iso-conversional method of Friedman. The amount of non-crystallizable, intra-molecular defects had substantial effects on the non-isothermal melt crystallization kinetics and subsequent melting behavior.

(Key-words: ethylene-acrylic acid copolymers; ethylene-methyl acrylate-acrylic acid terpolymers; non-isothermal melt crystallization kinetics; subsequent melting behavior)

¹ To whom correspondence should be addressed (E-mail address: manit.n@chula.ac.th)

² To whom correspondence should be addressed (E-mail address: pitt.s@chula.ac.th)

1. INTRODUCTION

For any material, its physical and mechanical properties are related directly to its structure and morphology. The structure and morphology of a semi-crystalline polymer are influenced by the conditions set forth during processing and control its ultimate physical and mechanical properties. Crystallization of a semi-crystalline polymer is still an on-going scientific pursuit, due largely to the important links crystallization has to processing conditions and the final properties of a product.

Ethylene-acrylic-acid copolymer (EAA) is a random copolymer made from ethylene monomer and acrylic acid co-monomer. The usefulness of EAA commercially arises from its combination of toughness, clarity, gloss, and adhesive ability to polar substrates [1]. Ethylene-methyl acrylate-acrylic acid terpolymer (E-MA-AA) is a random terpolymer consisting of ethylene monomer and methyl acrylate and acrylic acid co-monomers. E-MA-AA is commercialized by ExxonMobil Chemical under the tradename ESCOR™. Due to the presence of the co-monomers, E-MA-AA provides excellent adhesion to variety of both polar and non-polar substrates [2].

In the present contribution, the non-isothermal melt crystallization kinetics for four different grades of EAA and three different grades of E-MA-AA was investigated using differential scanning calorimetry (DSC) technique. The main objective for this work is to study the effect of co-monomer content on the crystallization behavior of these resins. The experimental data were analyzed based on the Ozawa and Ziabicki macrokinetic models. The effective energy barrier for non-isothermal melt crystallization process of these resins was estimated based on the differential iso-conversional method of Friedman.

2. THEORITICAL BACKGROUND

Ozawa [3] extended the well-known Avrami model [4-6] to describe the non-isothermal crystallization data of a semi-crystalline polymer. Mathematically, the relative crystallinity function of temperature $\theta(T)$ can be represented as a function of cooling rate (ϕ) as

$$\theta(T) = 1 - \exp\left(-\frac{k_o}{\phi^{n_o}}\right) \quad (1)$$

where k_o and n_o are the Ozawa crystallization rate constant and the Ozawa exponent, respectively. Both k_o and n_o are parameters specific to a given crystalline morphology and type of nucleation for a particular crystallization condition [7], similar to the kinetic parameters of the Avrami model. By plotting $\ln[-\ln(1-\theta(T))]$ versus $\ln(\phi)$ for a fixed temperature, both k_o and n_o parameters can be respectively determined from the anti-logarithmic value of the y-intercept (i.e., $k_o = e^{\text{y-intercept}}$) and the negative value of the slope (i.e., $n_o = -\text{slope}$) of a least-squared line drawn through the bulk of the data. Since the units of k_o are a function of n_o , use of K_o (i.e., $K_o = k_o^{1/n}$) is more favorable.

Instead of describing the crystallization process with complicated mathematical models, Ziabicki [8-10] proposed that the kinetics of polymeric phase transformation can be described by a first-order kinetic equation of the form:

$$\frac{d\theta(t)}{dt} = K_z(T)[1 - \theta(t)] \quad (2)$$

where $K_z(T)$ is a temperature-dependent crystallization rate function. In the case of non-isothermal crystallization, both $\theta(t)$ and $K_z(T)$ functions vary and are dependent on the cooling rate used.

For a given cooling condition, Ziabicki [8-10] showed that the crystallization rate function $K_z(T)$ can be described by a Gaussian function of the following form:

$$K_z(T) = K_{z,\max} \exp\left[-4 \ln 2 \frac{(T_c - T_{\max})^2}{D^2}\right] \quad (3)$$

where T_{\max} is the temperature at which the crystallization rate is maximum, $K_{z,\max}$ is the crystallization rate at T_{\max} , and D is the half-width of the crystallization rate-temperature function. With use of the isokinetic approximation, integration of

Equation (3) over the whole crystallizable range of temperatures ($T_g < T < T_m^0$), for a given cooling condition, leads to an important characteristic value describing the crystallization ability of a semi-crystalline polymer, namely, the kinetic crystallizability G_z :

$$G_z = \int_{T_g}^{T_m^0} K_z(T) dT \approx 1.064 K_{z,\max} D \quad (4)$$

In case of non-isothermal crystallization studies using DSC where cooling rate is a variable, Equation (4) can be applied when the crystallization rate function $K_z(T)$ is replaced with a derivative function of the relative crystallinity function of temperature $(d\theta/dT)_\phi$ specific for each cooling rate studied (i.e., crystallization rate function at different cooling rates). Therefore, Equation (4) is replaced by

$$G_{z,\phi} = \int_{T_g}^{T_m^0} (d\theta/dT)_\phi dT \approx 1.064 (d\theta/dT)_{\phi,\max} D_\phi \quad (5)$$

where $(d\theta/dT)_{\phi,\max}$ and D_ϕ are the maximum crystallization rate and the half-width of the derivative relative crystallinity as a function of temperature $(d\theta/dT)_\phi$. According to Equation (5), $G_{z,\phi}$ is the kinetic crystallizability at an arbitrary cooling rate ϕ . The kinetic crystallizability at unit cooling rate G_z can therefore be obtained by normalizing $G_{z,\phi}$ with ϕ (i.e., $G_z = G_{z,\phi}/\phi$). It should be noted that this procedure was first realized by Jeziorny [11].

For a process that occurs on cooling such as non-isothermal crystallization of polymer melts, reliable values of the effective energy barrier can be obtained, for examples, by the differential iso-conversional method of Friedman [12] or by the integral iso-conversional method of Vyazovkin [13,14]. In this work, the Friedman method will be used, due mainly to the reliability and simplicity of the method [14,15]. The Friedman equation is expressed as

$$\ln(\dot{\theta}_\theta(t)) = A - \frac{\Delta E_\theta}{RT} \quad (6)$$

where $\dot{\theta}_\theta(t)$ is the instantaneous crystallization rate as a function of time for a given relative melt conversion θ , A is an arbitrary pre-exponential parameter, and ΔE_θ is the effective energy barrier of the process for a given relative melt conversion θ . By plotting the instantaneous crystallization rate data measured from non-isothermal experiments conducted at various cooling rates against the corresponding inverse absolute temperature for a given conversion, the effective energy barrier for non-isothermal crystallization process can be determined.

3. EXPERIMENTAL DETAILS

3.1. Materials

Four grades of ethylene-acrylic acid copolymer (i.e., EAA1, EAA2, EAA4, and EAA5) and five grades of ethylene-methyl acrylate-acrylic acid terpolymer (i.e., E-MA-AA310, E-MA-AA320, and E-MA-AA325) with varying amount of the comonomer content were graciously supplied by ExxonMobil Chemical. Table 1 summarizes the compositions in mole fractions for EAA copolymers and E-MA-AA terpolymers. It should be noted that the melt-flow index of EAA4 is approximately twice that of EAA2.

3.2. Sample Preparation

All EAA and E-MA-AA resins were dried under vacuum at 50°C for 24 hours and kept in sealed plastic bags with silica gel prior to compression molding in order to minimize moisture absorption. Films of approximately 200 μm in thickness were prepared by melt-pressing the resins in a Wabash V50H compression molding machine using the plate temperature of 160°C and the applied force of 15 tons for 5 min. The compression molded films were then cooled to 40°C at a cooling rate which was fitted well by an exponential decay with a time constant of 3 min by running cold water through channels in the press plates. The thickness of film was ~200

3.3. Differential Scanning Calorimetry Measurements

A Perkin-Elmer Series 7 DSC was used to record non-isothermal melt crystallization exotherms and subsequent melting endotherms for these resins. Calibration for the temperature scale was carried out using a pure indium standard ($T_m^\circ = 156.6^\circ\text{C}$ and $\Delta H_f^\circ = 28.5 \text{ J}\cdot\text{g}^{-1}$) on every other run to ensure accuracy and reliability of the data obtained. To minimize thermal lag between the polymer sample and the DSC furnace, each sample holder was loaded with a disc-shape sample weighing around $9.0 \pm 0.1 \text{ mg}$ which was cut from the as-prepared films. It is worth noting that each sample was used only once and all the runs were carried out under nitrogen atmosphere to minimize extensive thermal degradation.

The experiment started with heating each sample from 30°C at a heating rate of $80^\circ\text{C}\cdot\text{min}^{-1}$ to 160°C . This procedure was aimed at nullifying previous thermal histories of the sample and at setting a standard thermal history to all of the samples studied. To ensure complete melting, the sample was kept at 160°C for 5 min, after which it was cooled at a desired cooling rate ϕ , ranging from 5 to $50^\circ\text{C}\cdot\text{min}^{-1}$ for EAA and from 5 to $30^\circ\text{C}\cdot\text{min}^{-1}$ for E-MA-AA, to 30°C . The sample was then subjected to heating to observe the subsequent melting behavior (recorded using a heating rate of $10^\circ\text{C}\cdot\text{min}^{-1}$). Both the non-isothermal melt crystallization exotherms and subsequent melting endotherms were recorded for further analysis. The non-isothermal melt crystallization exotherms were analyzed according to the models aforementioned.

4. RESULTS AND DISCUSSION

4.1. Non-Isothermal Melt Crystallization and Subsequent Melting Behavior.

The typical non-isothermal melt crystallization exotherms for EAA4 and E-MA-AA310 for indicated cooling rates are shown, for examples, in Figures 1a and 1b, respectively. It is obvious that, when the cooling rate increased, the exothermic trace became wider and shifted towards lower temperatures. The observation is universal for all of the EAA and E-MA-AA samples studied. Figure 2 illustrates, for examples, the non-isothermal crystallization exotherms recorded at a cooling rate of $10^\circ\text{C}\cdot\text{min}^{-1}$ for all of the EAA and E-MA-AA samples studied. Tables 2 and 3

summarize characteristic data for non-isothermal crystallization of all of the EAA and E-MA-AA samples studied. For each resin, the temperature at 1% relative crystallinity $T_{0.01}$, the temperature at the maximum crystallization rate (i.e., the peak temperature) T_p , and the temperature at 99% relative crystallinity $T_{0.99}$ were all shifted towards lower temperatures with increase cooling rate. The values of $T_{0.01}$ and $T_{0.99}$ will be hereafter used to as a measure of the beginning and the ending, respectively, of the non-isothermal crystallization process [7]. The fact that all of the $T_{0.01}$, T_p , and $T_{0.99}$ values decreased with increasing cooling rate suggests that the higher the cooling rate, the later the crystallization process began and ended (based on the temperature domain).

For a given cooling rate, the $T_{0.01}$, T_p , and $T_{0.99}$ values for all of the EAA and E-MA-AA samples studied fell on the following order: EAA1 > EAA2 > EAA4 > EAA5 > E-MA-AA310 > E-MA-AA320 > E-MA-AA325. The results suggest that EAA1 was the fastest to crystallize, while E-MA-AA325 was the slowest. This can be explained based on the amount of total non-crystallizable, intra-molecular defects (hereafter, co-monomer defects) that these resins exhibit. According to Table 1, EAA1, EAA2, EAA4, EAA5, E-MA-AA310, E-MA-AA320, and E-MA-AA325 resins show an increase in the amount of total co-monomer defects (in mole percentage) as 1.2, 2.6, 2.6, 3.9, 5.1, 9.8 and 10.7%, respectively. Since, these resins are random copolymers and terpolymers respectively, the increase in the amount of total co-monomer defects should result in a decrease in both the number and length of the crystallizable ethylene segments. As a consequence, for a given cooling condition, the resin having the lowest amount of total co-monomer defects (i.e., EAA1) should have the highest tendency for the crystallizable ethylene segments to overcome the energy barrier for crystallization to crystallize, as opposed to those with higher amount of total co-monomer defects. EAA2 and EAA4 have the same amount of non-crystallizable comonomers; the difference between these two materials is that the latter has a significantly lower molecular weight. Two competing effects occur in this situation, a lower molecular weight means a higher fraction of non-crystallizable chain ends, while a lower molecular weight also means higher mobility. Since the EAA2 crystallizes more readily, the former is more important than the latter for this material.

The subsequent melting endotherms for EAA4 and E-MA-AA310 after non-isothermally crystallized during cooling at various cooling rates are shown, for examples, in Figures 3a and 3b, respectively. It is apparent that, when the cooling rate increased, the melting endotherm became wider, while its peak position seems to be unchanged. The observation is similar to all of the EAA and E-MA-AA samples studied. Tables 3 and 4 summarize the enthalpy of crystallization ΔH_c (taken from the non-isothermal melt crystallization exotherms), the enthalpy of fusion ΔH_f , and the apparent melting temperature T_m (taken from the subsequent melting endotherms) for all of the EAA and E-MA-AA samples studied. Apparently for each resin, changes in the cooling rate used did not seem to affect the T_m value, while an increase in the cooling rate used resulted in a decrease in both ΔH_c and ΔH_f values. The latter observation suggests that the apparent degree of crystallinity was a decreasing function of the cooling rate.

For a given cooling rate, the ΔH_c , ΔH_f , and T_m values for all of the EAA and E-MA-AA samples studied followed the following sequence: EAA1 > EAA2 > EAA4 > EAA5 > E-MA-AA310 > E-MA-AA320 > E-MA-AA325. The results suggest that EAA1 exhibited the highest apparent degree of crystallinity and the thickest lamellae, while E-MA-AA325 showed the opposite. The explanation for such observation should lie, again, on the amount of total co-monomer defects or, in other words, the number and length of the crystallizable ethylene segments that these resins exhibit. For a given cooling condition, the resin with low amount of total co-monomer defects should have a better tendency to crystallize more perfectly, hence higher apparent degree of crystallinity and higher apparent melting temperature, than those with high amount of total co-monomer defects. The resin with high amount of total co-monomer defects (viz. the number and length of the crystallizable ethylene segments is respectively small and short) should show a broad melting endotherm, a direct result of a broad distribution of the lamellar thicknesses.

4.2. Non-Isothermal Melt Crystallization Kinetics

4.2.1 Ozawa Analysis

To obtain relevant non-isothermal melt crystallization kinetic information according to the Ozawa model, the experimental data such as those shown in Figure 1 need to be presented as the relative crystallinity function of temperature $\theta(T)$.

The conversion from the raw data, such as those shown in Figure 1, into the $\theta(T)$ can be carried out using the following equation:

$$\theta(T) = \frac{\int_{T_o}^T \left(\frac{dH_c}{dT} \right) dT}{\Delta H_c} \quad (7)$$

where T_o represents the temperature corresponding to the onset of crystallization, dH_c is the enthalpy of crystallization released during an infinitesimal temperature range dT , and ΔH_c is the overall enthalpy of crystallization for a specific cooling condition.

Typical relative crystallinity functions of temperature $\theta(T)$ are shown in Figure 4. The fact that the $\theta(T)$ function for a given resin shifted towards lower temperatures with cooling rate confirms our earlier observation that the higher the cooling rate, the later the crystallization process began and ended. It was mentioned previously that analysis of the raw $\theta(T)$ data could be carried out by performed through a double logarithmic plot of $\ln[-\ln(1-\theta(T))]$ versus $\ln(\phi)$ for a fixed temperature. Figures 5a and 5b illustrate plots of $\ln[-\ln(1-\theta(T))]$ versus $\ln(\phi)$ for a fixed temperature based on data shown in Figures 4a and 4b. Tables 6 and 7 summarize the n_o and K_o values as well as the corresponding correlation coefficient r^2 of the fit for all of the EAA and E-MA-AA samples studied. It should be noted that the results were only taken from least-squared lines drawn through plots of at least three points was the main reason for the variation in the temperature range used for different resins.

The values of the correlation coefficients r^2 listed in Tables 6 and 7 which were found to range from 0.8496 to 0.9954 suggesting that the Ozawa model provided a satisfactory description to the non-isothermal melt crystallization for these resins. In all cases, the Ozawa exponent n_o was found to range from ca. 2.1 to 5.3. More specifically, it ranged from ca. 3.4 to 4.4 for EAA1 within the temperature range of 77 to 85°C, from ca. 3.2 to 4.3 for EAA2 within the temperature range of 73 to 81°C, from ca. 3.5 to 4.6 for EAA4 within the temperature range of 73 to 81°C, from ca. 3.3 to 3.6 for EAA5 within the temperature range of 67 to 75°C, from ca. 3.3 to 3.5 for E-MA-AA310 within the temperature range of 63 to 71°C, from ca. 4.2 to 5.3 for E-MA-AA320 within the temperature range of 45 to 53°C, and from ca. 2.1 to 3.8 for E-MA-AA325 within the temperature range of 39 to 47°C. For all of the EAA and E-MA-AA samples studied, the Ozawa crystallization rate constant K_o was found to decrease with increasing temperature (within the temperature range investigated), suggesting that these resins crystallized slower with increasing temperature.

4.2.2. Ziabicki's Kinetic Crystallizability Analysis

Analysis according to the modified first order Ziabicki's kinetic equation (i.e., Equation 5) can be carried out by differentiating the relative crystallinity function of temperature $\theta(T)$, i.e. the data in Figure 4, in order to obtain the derivative relative crystallinity as a function of temperature $(d\theta/dT)_\phi$. Once the $(d\theta/dT)_\phi$ function is obtained, various kinetic parameters (i.e., the maximum crystallization rate $(d\theta/dT)_{\phi,\max}$ and the half-width of the $(d\theta/dT)_\phi$ function D_ϕ) can then be obtained and the cooling rate-dependent kinetic crystallizability $G_{z,\phi}$ can be calculated according to Equation (5).

Tables 8 and 9 summarize the values of $T_{\phi,\max}$ (i.e., the temperature at the maximum crystallization rate as determined from the $(d\theta/dT)_\phi$ functions), $(d\theta/dT)_{\phi,\max}$, D_ϕ and G_z for all of the EAA and E-MA-AA samples studied. It should be noted that the values of $T_{\phi,\max}$ listed in Tables 8 and 9 and T_p (i.e., the temperature at the maximum crystallization rate as determined from the raw non-isothermal melt crystallization exotherms) listed in Tables 2 and 3 are almost identical for all of the

resins studied. For a given resin, the $T_{\phi, \max}$ value was found to decrease, while the $(d\theta/dT)_{\phi, \max}$ and D_{ϕ} values were also found to increase, with increasing cooling rate. Based on these values, the resulting $G_{z, \phi}$ value (not listed) was therefore an increasing function of the cooling rate. After normalizing the effect of the cooling rate from the resulting $G_{z, \phi}$ value, the value of the kinetic crystallizability at unit cooling rate G_z can therefore be determined and the results shown in Tables 8 and 9 confirmed that the normalized G_z values for each resin at different cooling rates were almost identical. However, The kinetic crystallizability at unit cooling rate G_z slightly decreased when the amount of total defect was increased.

Since the physical meaning of the kinetic crystallizability G_z is to characterize the ability for a semi-crystalline polymer in crystallizing when it is cooled from its equilibrium melting temperature to the glass transition temperature at a unit cooling rate, the higher the G_z value, the more readily the polymer crystallizes. Based on the average G_z values summarized in Tables 8 and 9, the crystallization ability for all of the EAA and E-MA-AA samples studied followed the following order: EAA1 > EAA4 > EAA2 > EAA5 \approx E-MA-AA310 > E-MA-AA320 > E-MA-AA325, which is slightly different from previous observation.

4.2.3. Effective Energy Barrier for Non-Isothermal Melt Crystallization Process

In order to estimate the effective energy barrier for non-isothermal melt crystallization process ΔE for these polymers according to the differential iso-conversional method of Friedman [12], the relative crystallinity function of temperature $\theta(T)$, such as those shown in Figure 4, needs to be converted to the relative crystallinity function of time $\theta(t)$ by transforming the horizontal temperature axis into the time axis, using the relationship between the crystallization time t and the sample temperature T according to the following equation:

$$t = \frac{T_0 - T}{\phi} \quad (8)$$

Once the $\theta(t)$ function is obtained, it is differentiated to obtain the instantaneous crystallization rate as a function of time derivative relative crystallinity as a function of time $\dot{\theta}(t)$. Finally, a plot according to Equation (6) can be performed for various values of relative melt conversion (i.e., relative crystallinity) using the data obtained from the $\dot{\theta}(t)$ and $\theta(T)$ functions and, finally, the effective energy barrier of the non-isothermal melt crystallization process for a given relative melt conversion θ (i.e., ΔE_{θ}) can be estimated from the slope of the plot (i.e., $\Delta E_{\theta} = -(\text{slope})(R)$).

Tables 10 and 11 summarize the ΔE_{θ} values determined for 5 different values of θ ranging from 0.1 to 0.9 for all of the EAA and E-MA-AA samples studied. According to Tables 10 and 11, the ΔE value for each resin was found to monotonically increased with increasing relative melt conversion, suggesting that, as the crystallization progressed, it was more difficult for the polymer to crystallize. As crystallization proceeds, diffusion of the crystallizing molecular segments from the melt to the growth front will be deterred by the rejected molecular segments. For a given value of θ , the ΔE values for all of the EAA and E-MA-AA samples studied were found to lie in the following order: EAA1 < EAA2 < EAA4 < EAA5 < E-MA-AA310 < E-MA-AA320 < E-MA-AA325. The results suggest that EAA1 was the easiest resin to crystallize, while E-MA-AA325 was the most difficult one to do so. The different amounts of total co-monomer defects that these resins exhibited was, again, responsible for such behavior.

5. CONCLUSIONS

The non-isothermal melt crystallization exotherms for four grades of ethylene-acrylic acid copolymer (EAA) and three grades of ethylene-methyl acrylate-acrylic acid terpolymers (E-MA-AA) showed that the temperature at 1% relative crystallinity, the temperature at the maximum crystallization rate, and the temperature at 99% relative crystallinity were all shifted towards lower temperatures with an increase in cooling rate used, indicating that these resins took a shorter time to crystallize when the cooling rate increased. The Ozawa model was found to provide a satisfactorily good fit to the experimental data. For all of the resins studied, the Ozawa exponent was found to range from ca. 2.1 to 5.3 and the Ozawa

crystallization rate constant was found to decrease with increasing temperature (within the temperature range investigated), suggesting that these resins crystallized slower with increasing temperature.

The comparative ability for these resins to crystallize from the molten state under a unit cooling rate can be evaluated from the values of the Ziabicki's kinetic crystallizability, which suggested that the ability for these resins to crystallize fell on the following order: EAA1 > EAA4 > EAA2 > EAA5 \approx E-MA-AA310 > E-MA-AA320 > E-MA-AA325. However, when judging from the observation of the raw non-isothermal melt crystallization exotherms and the values of the effective energy barrier governing the non-isothermal melt crystallization for these resins, the ability for these resins to crystallize was in the following sequence: EAA1 > EAA2 > EAA4 > EAA5 > E-MA-AA310 > E-MA-AA320 > E-MA-AA325. It was postulated that the amount of co-monomer defects was responsible for such behavior.

ACKNOWLEDGMENTS

The authors wish to thank ExxonMobil Chemical Company, and in particular Dr. Joe Domine, for supply of ethylene-acrylic acid copolymers and ethylene-methyl acrylate-acrylic acid terpolymers used in this study. MN and PS acknowledges a grant provided by Chulalongkorn University through the Development Grants for New Faculty/Researchers. Partial support from the Petroleum and Petrochemical Technology Consortium and the Petroleum and Petrochemical College is also greatly acknowledged.

REFERENCES

- [1] N Pongrakananon, N Somrang, W Visitsart, P Supaphol, M Nithitanakul, and BP Grady, *J Appl Polym Sci*, submitted.
- [2] <http://www.exxonmobilchemical.com>
- [3] T Ozawa, *Polymer* 1971, 12, 150.
- [4] M Avrami, *J Chem Phys* 1939, 7, 1103.
- [5] M Avrami, *J Chem Phys* 1940, 8, 212.
- [6] M Avrami, *J Chem Phys* 1941, 9, 177.
- [7] B Wunderlich, in "Macromolecular Physics," Vol.2, Academic Press, New York, 1976, p 147.
- [8] A Ziabicki, *Appl Polym Symp* 1967, 6, 1.
- [9] A Ziabicki, *Polymery* 1967, 12, 150.
- [10] A Ziabicki, In "Fundamentals of Fiber Spinning," John Wiley & Sons, New York 1976, pp 112-114.
- [11] A Jeziorny, *Polymer* 1978, 19, 1142.
- [12] H Friedman, *J Polym Sci* 1964, C6, 183.
- [13] S Vyazovkin, *J Comput Chem* 1997, 18, 393.
- [14] S Vyazovkin, *J Comput Chem* 2001, 22, 178.
- [15] S Vyazovkin, *Macromol Rapid Commun* 2002, 23, 771.

CAPTIONS OF FIGURES

- Figure 1. Non-isothermal crystallization exotherms for (a) EAA4 and (b) E-MA-AA310 at various cooling rates.
- Figure 2. Non-isothermal crystallization exotherms for (a) four grades of EAA and (b) three grades of E-MA-AA at the cooling rate of $10^{\circ}\text{C}\cdot\text{min}^{-1}$.
- Figure 3. Subsequent melting endotherms of EAA4 for (a) EAA4 and (b) E-MA-AA310 after non-isothermally crystallized at various cooling rates.
- Figure 4. The relative crystallinity function of temperature for (a) EAA4 and (b) E-MA-AA310 at various cooling rates.
- Figure 5. Typical Ozawa analysis based on the non-isothermal crystallization data of (a) EAA4 and (b) E-MA-AA310.

Table 1 Compositions in mole fractions for EAA copolymers and E-MA-AA terpolymers studied

Sample code	Ethylene	Acrylic acid	Methyl acrylate
EAA1	0.988	0.012	-
EAA2	0.974	0.026	-
EAA4*	0.974	0.026	-
EAA5	0.961	0.039	-
E-MA-AA310	0.949	0.028	0.023
E-MA-AA320	0.902	0.028	0.070
E-MA-AA325	0.893	0.028	0.079

* EAA4 has lower molecular weight averages than EAA2

Table 2 Characteristic data of non-isothermal melt crystallization exotherms for EAA copolymers studied

ϕ (°C·min ⁻¹)	EAA1			EAA2			EAA4			EAA5		
	$T_{0.01}$ (°C)	T_p (°C)	$T_{0.99}$ (°C)	$T_{0.01}$ (°C)	T_p (°C)	$T_{0.99}$ (°C)	$T_{0.01}$ (°C)	T_p (°C)	$T_{0.99}$ (°C)	$T_{0.01}$ (°C)	T_p (°C)	$T_{0.99}$ (°C)
5	90.1	87.4	84.6	86.0	83.5	80.7	84.4	81.9	79.4	79.8	76.2	73.0
10	87.5	84.8	80.8	83.8	81.0	76.5	82.6	79.0	74.9	76.8	72.5	68.7
15	85.9	83.2	78.9	82.2	79.0	74.1	81.0	77.5	73.2	75.7	70.7	65.6
20	84.5	81.9	77.7	80.7	77.3	72.6	79.1	75.3	70.1	74.3	74.5	64.4
30	81.9	78.9	71.4	77.6	73.9	66.5	76.6	71.9	65.5	71.0	65.9	59.1
40	79.9	76.5	68.1	75.4	71.2	62.1	73.8	69.2	59.7	68.3	61.9	54.7
50	76.2	71.8	60.7	72.4	67.3	57.8	69.4	63.3	53.0	61.0	53.8	45.5

Table 3 Characteristic data of non-isothermal melt crystallization exotherms for E-MA-AA terpolymers studied

ϕ (°C·min ⁻¹)	E-MA-AA310			E-MA-AA320			E-MA-AA325		
	$T_{0.01}$ (°C)	T_p (°C)	$T_{0.99}$ (°C)	$T_{0.01}$ (°C)	T_p (°C)	$T_{0.99}$ (°C)	$T_{0.01}$ (°C)	T_p (°C)	$T_{0.99}$ (°C)
5	75.8	73.2	69.7	59.0	55.2	49.5	53.0	49.6	45.3
10	74.0	71.0	65.1	55.5	51.9	45.5	50.6	46.5	41.5
15	72.5	69.3	62.8	52.8	49.6	43.7	47.5	43.9	37.6
20	70.7	67.1	60.9	51.9	47.9	40.2	46.0	41.4	35.7

Table 4 Enthalpy of crystallization and characteristic data of subsequent melting endotherms for EAA copolymers studied

ϕ (°C·min ⁻¹)	EAA1			EAA2			EAA4			EAA5		
	ΔH_c (J·g ⁻¹)	ΔH_f (J·g ⁻¹)	T_m (°C)	ΔH_c (J·g ⁻¹)	ΔH_f (J·g ⁻¹)	T_m (°C)	ΔH_c (J·g ⁻¹)	ΔH_f (J·g ⁻¹)	T_m (°C)	ΔH_c (J·g ⁻¹)	ΔH_f (J·g ⁻¹)	T_m (°C)
5	67.6	86.8	101.2	53.6	80.8	98.2	49.9	67.8	97.0	51.8	64.2	93.4
10	65.2	85.4	101.4	53.8	68.3	98.0	52.8	58.4	96.9	51.0	52.9	94.0
15	68.7	81.2	100.7	65.7	67.7	97.3	62.1	44.2	96.7	50.1	48.0	94.3
20	57.9	68.7	99.9	75.9	79.2	97.4	78.2	37.0	96.7	52.3	60.1	94.0
30	58.1	69.5	99.9	61.9	65.8	97.3	55.7	56.1	96.8	51.1	46.2	94.3
40	58.3	74.1	99.9	56.4	59.6	97.2	61.2	53.9	97.2	50.4	46.0	94.2
50	59.6	59.7	100.6	51.4	52.6	97.1	63.3	54.0	97.4	47.1	48.0	94.7

Table 5 Enthalpy of crystallization and characteristic data of subsequent melting endotherms for E-MA-AA terpolymers studied.

ϕ (°C·min ⁻¹)	E-MA-AA310			E-MA-AA320			E-MA-AA325		
	ΔH_c (J·g ⁻¹)	ΔH_f (J·g ⁻¹)	T_m (°C)	ΔH_c (J·g ⁻¹)	ΔH_f (J·g ⁻¹)	T_m (°C)	ΔH_c (J·g ⁻¹)	ΔH_f (J·g ⁻¹)	T_m (°C)
5	38.9	46.4	88.2	20.6	22.7	73.5	18.2	16.4	68.5
10	37.6	39.3	89.5	19.3	13.1	70.3	21.0	15.0	69.2
15	33.0	36.4	89.7	30.3	16.5	72.0	17.2	9.0	68.9
20	33.5	27.7	87.2	20.9	13.7	73.0	17.9	9.6	68.6

Table 6 Non-isothermal crystallization kinetics for EAA copolymers based on Ozawa analysis

EAA1				EAA2				EAA4				EAA5			
Temperature	n_o	K_o	r^2	Temperature	n_o	K_o	r^2	Temperature	n_o	K_o	r^2	Temperature	n_o	K_o	r^2
(°C)		(°C·min ⁻¹)		(°C)		(°C·min ⁻¹)		(°C)		(°C·min ⁻¹)		(°C)		(°C·min ⁻¹)	
77	3.74	31.82	0.9928	73	4.32	28.39	0.9894	73	3.69	20.92	0.8551	67	3.32	23.56	0.9430
79	4.39	23.41	0.9335	75	3.92	19.66	0.8678	75	3.53	17.34	0.9222	69	3.31	17.07	0.9329
81	3.70	16.88	0.9078	77	4.22	16.19	0.8711	77	3.57	13.41	0.9346	71	3.40	10.97	0.8702
83	3.43	12.90	0.9038	79	3.61	13.00	0.9818	79	4.07	8.37	0.8992	73	3.31	8.90	0.9481
85	3.49	7.74	0.8496	81	3.16	8.11	0.9801	81	4.63	5.87	0.9640	75	3.61	5.90	0.9954

Table 7 Non-isothermal crystallization kinetics for E-MA-AA terpolymers based on Ozawa analysis

E-MA-AA310				E-MA-AA320				E-MA-AA325			
Temperature	n_o	K_o	r^2	Temperature	n_o	K_o	r^2	Temperature	n_o	K_o	r^2
(°C)		(°C·min ⁻¹)		(°C)		(°C·min ⁻¹)		(°C)		(°C·min ⁻¹)	
63	3.48	34.26	0.8567	45	4.23	21.24	0.8667	39	2.12	32.57	0.9741
65	3.34	27.24	0.8667	47	5.19	17.99	0.9928	41	2.59	15.30	0.8567
67	3.32	23.56	0.9928	49	4.98	13.21	0.9335	43	2.26	13.61	0.8667
69	3.31	17.07	0.9335	51	4.25	10.08	0.9078	45	3.16	11.32	0.9928
71	3.40	10.97	0.9078	53	5.26	6.20	0.9038	47	3.79	6.32	0.9335

Table 8 Non-isothermal crystallization kinetics for EAA copolymers based on Ziabicki analysis

ϕ (°C·min ⁻¹)	EAA1				EAA2				EAA4				EAA5				
	$T_{\phi,\max}$ (°C)	$(d\theta/dT)_{\phi,\max}$ s ⁻¹	D_{ϕ} (°C)	G_z	$T_{\phi,\max}$ (°C)	$(d\theta/dT)_{\phi,\max}$ s ⁻¹	D_{ϕ} (°C)	G_z	$T_{\phi,\max}$ (°C)	$(d\theta/dT)_{\phi,\max}$ s ⁻¹	D_{ϕ} (°C)	G_z	$T_{\phi,\max}$ (°C)	$(d\theta/dT)_{\phi,\max}$ s ⁻¹	D_{ϕ} (°C)	G_z	
5	87.4	2.85x10 ⁻²	10.03	3.65	83.5	2.74x10 ⁻²	7.49	2.62	81.9	2.86x10 ⁻²	10.02	3.66	76.2	2.10x10 ⁻²	10.03	2.69	
10	84.8	4.67x10 ⁻²	12.52	3.73	81.0	4.49x10 ⁻²	10.06	2.88	79.0	3.91x10 ⁻²	10.71	2.67	72.5	3.67x10 ⁻²	12.52	2.93	
15	83.0	6.31x10 ⁻²	13.41	3.60	79.0	5.88x10 ⁻²	12.45	3.11	77.5	5.70x10 ⁻²	12.92	3.13	70.7	4.61x10 ⁻²	14.53	2.85	
20	81.9	8.82x10 ⁻²	14.68	4.13	77.6	7.42x10 ⁻²	15.08	3.57	75.3	6.94x10 ⁻²	15.72	3.48	69.3	6.38x10 ⁻²	15.59	3.18	
30	78.9	9.32x10 ⁻²	19.61	3.89	73.9	8.36x10 ⁻²	19.15	3.40	72.4	8.31x10 ⁻²	17.57	3.10	65.9	7.84x10 ⁻²	19.64	3.28	
40	76.5	10.76x10 ⁻²	22.43	3.85	71.2	9.27x10 ⁻²	21.40	3.17	69.2	9.00x10 ⁻²	21.38	3.07	61.9	8.43x10 ⁻²	24.67	3.32	
50	67.3	11.38x10 ⁻²	24.35	3.54	67.3	10.77x10 ⁻²	22.30	3.07	83.3	9.81x10 ⁻²	27.31	3.42	53.3	8.68x10 ⁻²	25.90	2.87	
			Average	3.77			Average	3.12				Average	3.22			Average	3.02

Table 9 Non-isothermal crystallization kinetics for E-MA-AA terpolymers based on Ziabicki analysis

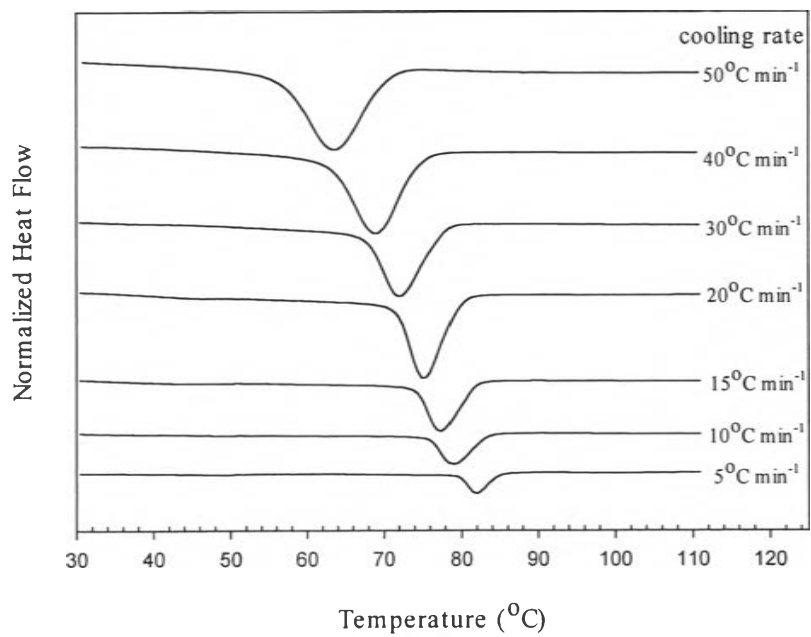
ϕ ($^{\circ}\text{C}\cdot\text{min}^{-1}$)	E-MA-AA310				E-MA-AA320				E-MA-AA325			
	$T_{\phi,\text{max}}$ ($^{\circ}\text{C}$)	$(d\theta/dT)_{\phi,\text{max}}$ s^{-1}	D_{ϕ} ($^{\circ}\text{C}$)	G_z	$T_{\phi,\text{max}}$ ($^{\circ}\text{C}$)	$(d\theta/dT)_{\phi,\text{max}}$ s^{-1}	D_{ϕ} ($^{\circ}\text{C}$)	G_z	$T_{\phi,\text{max}}$ ($^{\circ}\text{C}$)	$(d\theta/dT)_{\phi,\text{max}}$ s^{-1}	D_{ϕ} ($^{\circ}\text{C}$)	G_z
5	73.2	2.35×10^{-2}	7.53	2.26	55.2	1.62×10^{-2}	11.62	2.40	49.5	1.87×10^{-2}	7.53	1.79
10	70.9	4.02×10^{-2}	12.43	3.19	51.8	3.22×10^{-2}	14.08	2.90	46.4	3.20×10^{-2}	10.22	2.09
15	69.3	5.54×10^{-2}	13.26	3.13	49.5	4.99×10^{-2}	16.85	3.58	43.8	4.90×10^{-2}	11.55	2.41
20	67.1	6.12×10^{-2}	14.41	2.83	47.8	5.62×10^{-2}	15.29	2.74	41.3	5.68×10^{-2}	12.30	2.23
30	64.1	9.44×10^{-2}	18.28	3.67	42.1	6.18×10^{-2}	17.17	2.26	-	-	-	-
		Average		3.02		Average		2.78		Average		2.13

Table 10 Effective energy barrier describing the overall non-isothermal melt crystallization of EAA copolymers based on Friedman method

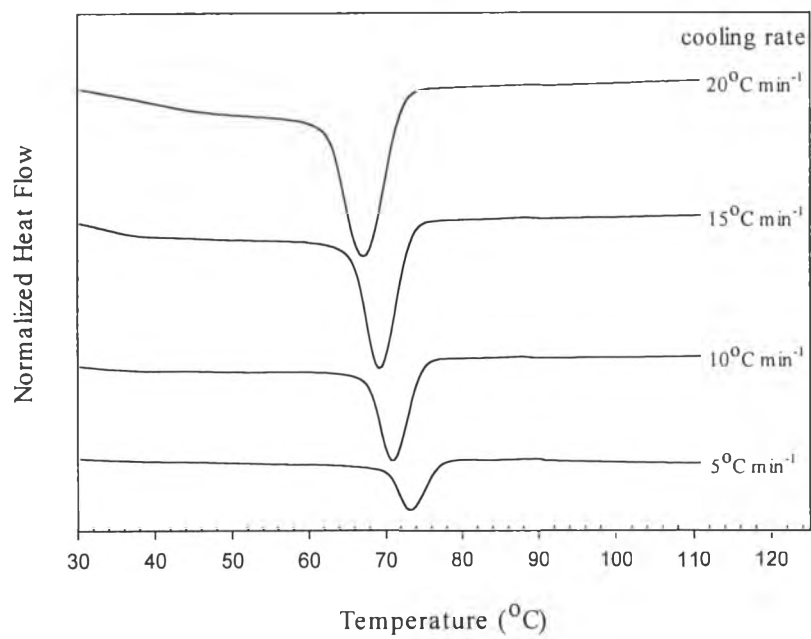
Polymer	Effective energy barrier ΔE (kJ·mol ⁻¹)				
	$\theta = 0.1$	$\theta = 0.3$	$\theta = 0.5$	$\theta = 0.7$	$\theta = 0.9$
EAA1	-258.0	-226.7	-209.0	-205.6	-157.0
EAA2	-208.7	-198.1	-166.2	-153.2	-141.2
EAA4	-162.1	-145.8	-128.1	-125.4	-112.3
EAA5	-146.8	-138.0	-127.4	-112.8	-86.8

Table 11 Effective energy barrier describing the overall non-isothermal melt crystallization of E-MA-AA terpolymers based on Friedman method

Polymer	Effective energy barrier ΔE (kJ·mol ⁻¹)				
	$\theta = 0.1$	$\theta = 0.3$	$\theta = 0.5$	$\theta = 0.7$	$\theta = 0.9$
E-MA-AA310	-132.2	-114.2	-104.9	-103.6	-96.7
E-MA-AA320	-100.2	-93.4	-88.8	-81.4	-82.8
E-MA-AA325	-97.6	-90.6	-88.7	-73.0	-62.7

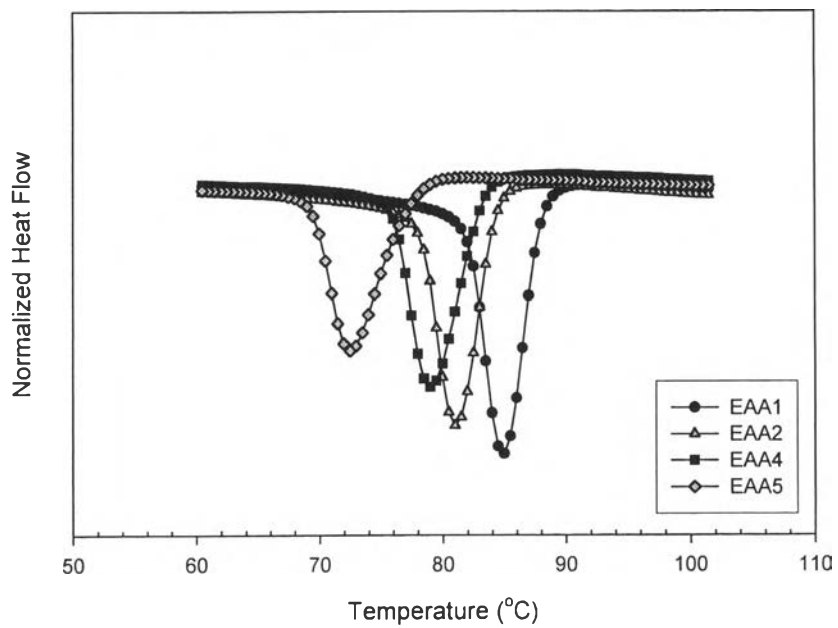


(a)

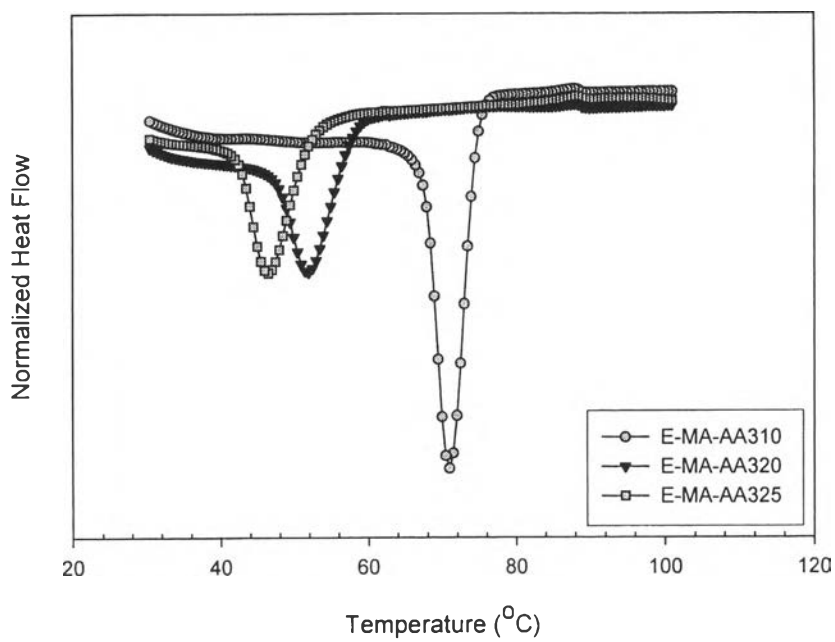


(b)

Figure 1

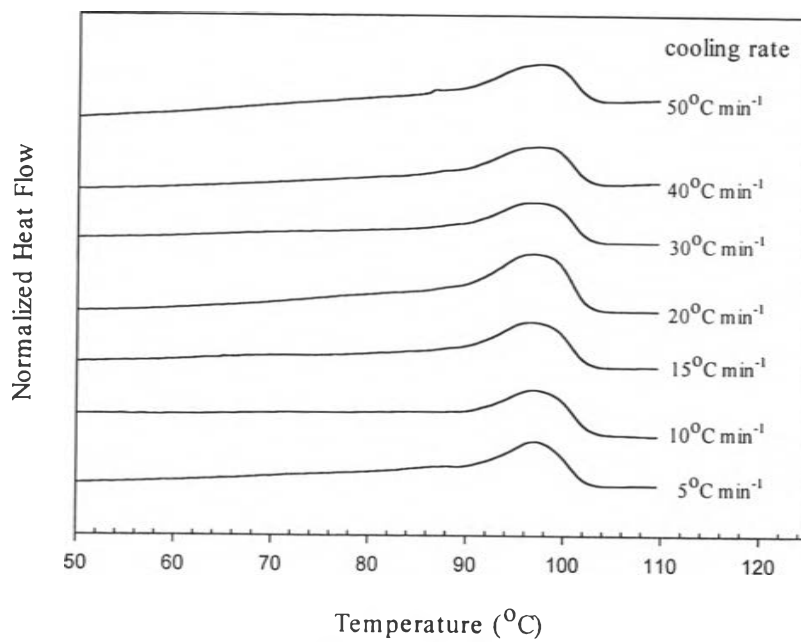


(a)

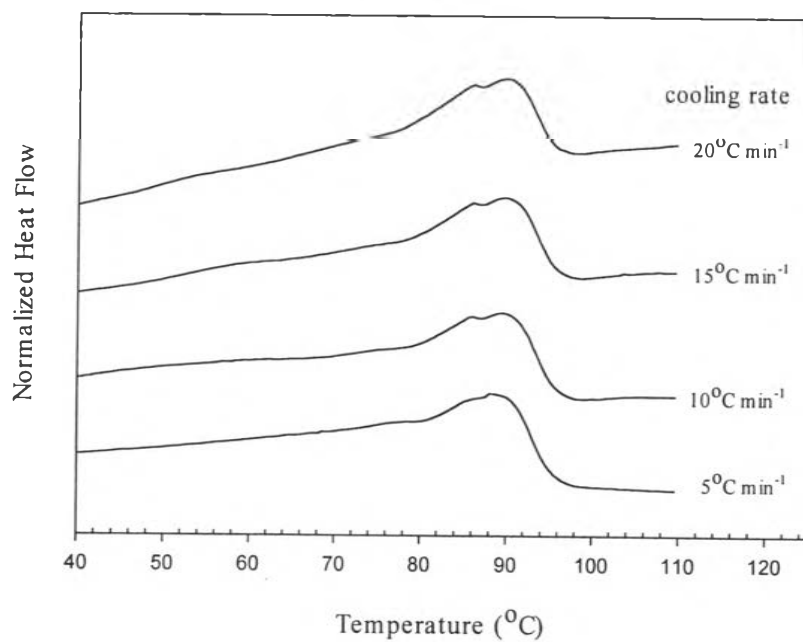


(b)

Figure 2

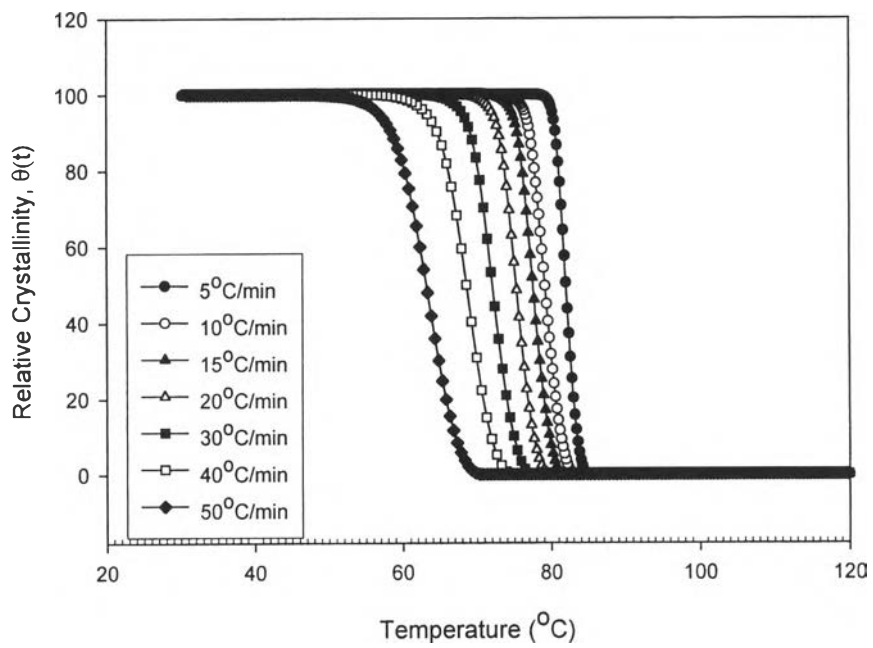


(a)

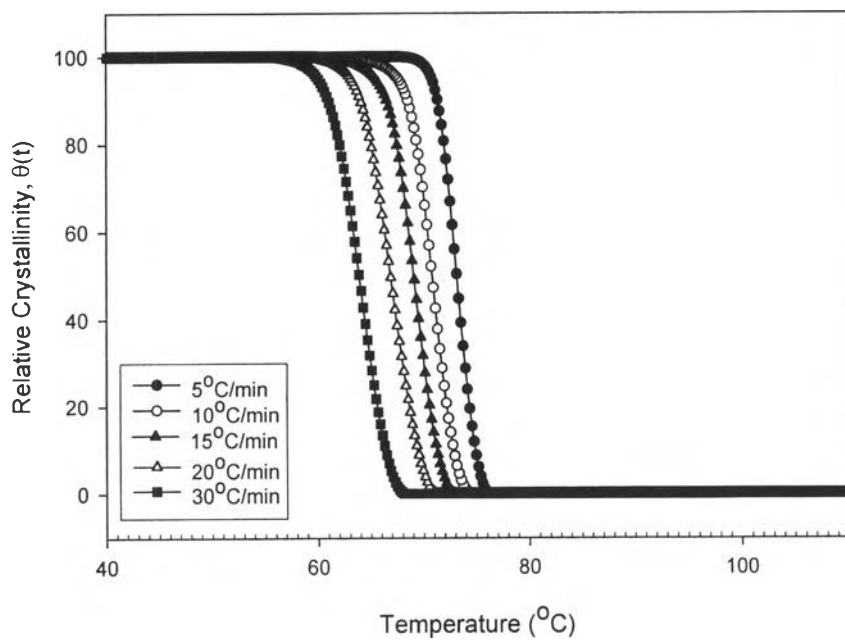


(b)

Figure 3

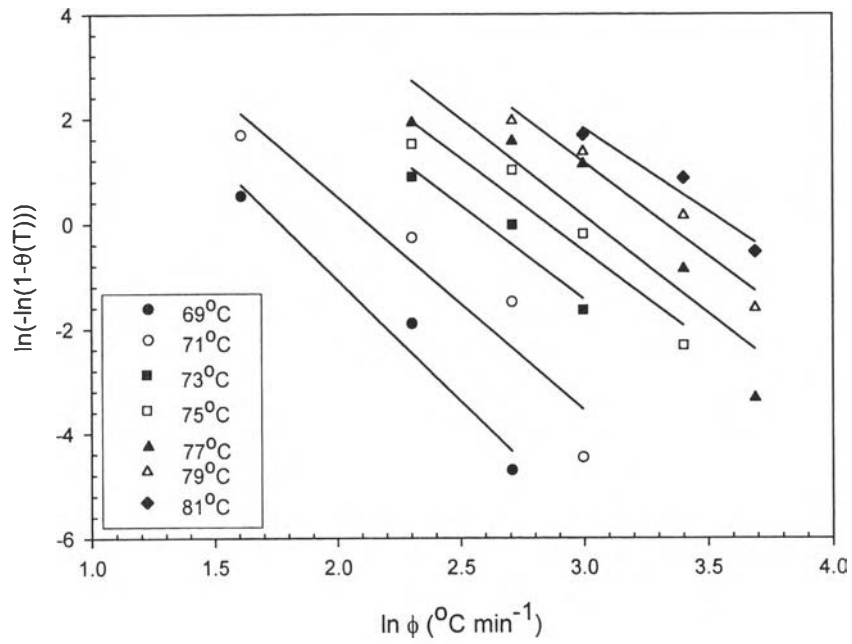


(a)

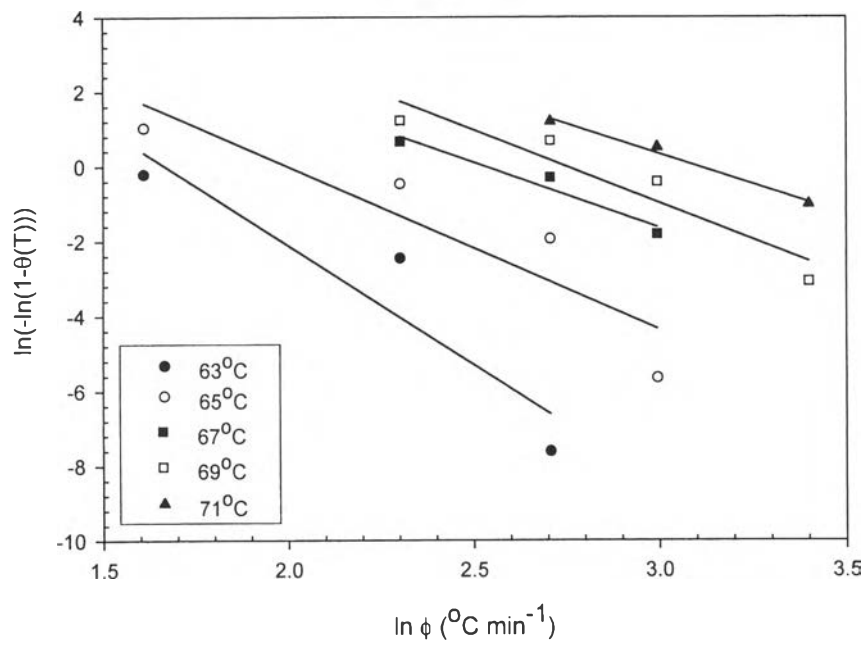


(b)

Figure 4



(a)



(b)

Figure 5